11th World Congress on Computational Mechanics (WCCM XI)
5th European Conference on Computational Mechanics (ECCM V)
6th European Conference on Computational Fluid Dynamics (ECFD VI)
E. Oñate, J. Oliver and A. Huerta (Eds)

STUDY OF ENERGY HARVESTING FROM TRAFFIC-INDUCED BRIDGE VIBRATIONS

Dominique Siegert*,**Michaël Peigney**†

* Université Paris-Est, IFSTTAR/COSYS, F-77455 Marne-la-Valle Cedex 2, France
e-mail: dominique.siegert@ifsttar.fr
† Université Paris-Est, Laboratoire Navier (Ecole des Ponts ParisTech, IFSTTAR, CNRS),
F-77455 Marne-la-Valle Cedex 2, France
e-mail: michael.peigney@polytechnique.org

Key words: energy harvesting, bridge vibrations, piezoelectricity

Abstract. This paper focuses on energy harvesting of traffic-induced vibrations in bridges. Using a pre-stressed concrete highway bridge as a case study, in situ vibration measurements are presented and analyzed. From those results, a prototype of cantilever piezoelectric harvester was designed, tested, and modeled. Even though the considered bridge vibrations are characterized by small amplitude and a low frequency (i.e. below 15 Hz), it is shown that mean power of the order of 0.03 mW can be produced, with a controlled voltage between 1.8 and 3.6 V. A simple model is proposed for the theoretical prediction of the delivered power in terms of traffic intensity. That model shows good agreement with the experimental results and leads to a simple but effective design rule for piezoelectric harvesters to be used on bridges.

1 INTRODUCTION

The design of piezoelectric or inductive energy harvesters usually targets small size inertial oscillators weighting less than a few grams with resonant frequencies above 30 Hz [1]. Such high frequencies can be found in vibrations of machine tools, which are characterized by peak accelerations in the range 1-10 $\mathrm{m.s}^{-2}$ at frequencies between 70 Hz and 120 Hz.

This paper focuses on using bridge vibrations as an energy source for self powered health monitoring sensor node [2, 3, 4]. As traffic-induced bridge vibrations are low frequency and have small amplitudes, energy harnessing is challenging even for measuring slow time varying signal such as temperature or humidity.

More precisely, the present works aims at giving a deeper insight into the traffic induced vibration characteristics measured on a bridge at different source locations. For the bridge example considered, the predicted performances of a validated model of piezoelectric harvesting device are subsequently discussed in relation with the traffic intensity.

2 TRAFFIC INDUCED BRIDGE VIBRATION MEASUREMENTS

2.1 Case study

Traffic induced vibrations have been measured on a prestressed concrete highway bridge located on a heavily trafficked itinerary in the north of France (Figure 1). A 33 m long simply supported span carrying three one way lanes has been instrumented with 4 accelerometers. The structure consists of five cross braced girders as shown in Figures 1-2(left).From traffic data delivered by the ministry of transport, the mean flow of heavy lorries was about 8000 per day with large variations according to the day of the week and time in the day. Weigh-in-motion (WIM) data recorded in 2004 has shown that a high traffic intensity corresponds to 400 lorries per hour [5].

Figure 1: Bridge considered in the study.

Figure 2: Bridge superstructure (left) and view of a water pipe on girder 1 (right).

The work in [5] was dealing with the traffic effects on this particular bridge. It was noticed that the vehicle-bridge dynamic interaction was sensitive to the characteristics of

the vehicle suspension. Negligible dynamic effects were observed on the measured strain responses for most of the moving five axles semi-trailer vehicles. For that type of lorry (which represented 80 % of the heavy gross weight lorries population crossing the bridge), the weak dynamic impact factor on small span bridges was attributed to the pneumatic system in the vehicle suspension.

2.2 Time-domain analysis of vibration measurements

Acceleration time series were measured with a sampled frequency of 300 Hz on girders 1 and 3 of the simply supported span at three locations shown in Figure 3. An example of recorded acceleration signal is displayed in Figure 4. For a high traffic intensity, the root mean square value of the measured acceleration at mid-span on girder 1 – which is more heavily loaded – was as low as 0.03 m.s^{-2}. Significantly higher levels of vibration were measured on a water pipe fixed on the girder 1 (see Figure 2(right)). An example of acceleration time series recorded on that pipe is displayed in Figure 4. The root mean square value of the measured acceleration for a high traffic intensity was 0.3 m.s^{-2}, ten times the estimated value on the girder. For low traffic intensity, the root mean square value of acceleration decreased to 0.1 m.s^{-2}. These estimates give the expected range of acceleration to be considered for this ambient source of vibration.

An observation of importance for our purpose is that the measured acceleration signal consists of successive short-time pulses, each pulse corresponding to an individual lorry crossing the bridge. This is especially clear in night time, for which traffic intensity is low enough for an inter-arrival time to exceed the time to cross the bridge (see Figure 5) . The calculated average duration of the pulse was 2 s, which corresponds to the time for a five axles semi-trailer vehicle to cross the span of the bridge in free flowing traffic conditions. The average acceleration peak level was 0.58 m.s^{-2}. In high traffic conditions, there is some overlap between the excitations due to each lorry, resulting in a signal that is more difficult to interpret (Figure 4). Light vehicles produces a low-level signal (ambient noise) with no discernible structure.

2.3 Frequency-domain analysis of vibration measurements

A spectral analysis of the recorded signals was performed in order to determine the frequency content of the vibration sources on the bridge. Smoothed power spectra of the acceleration responses to the traffic excitation were estimated by averaging 360 power spectra of 3000 samples blocks. Three main resonant frequencies of the bridge deck were identified in the frequency range from 0 to 50 Hz. Two close frequencies were in the vicinity of 4 Hz and an other one was found at 14.5 Hz (Figure 6). The results of a previous experimental modal analysis [6] carried out with a stochastic subspace identification method (SSI) have shown that the two close frequencies were located at 3.9 Hz and 4.3 Hz. These resonant frequencies correspond to the longitudinal bending, torsional and transversal bending deformations of the deck bridge. Those experimental

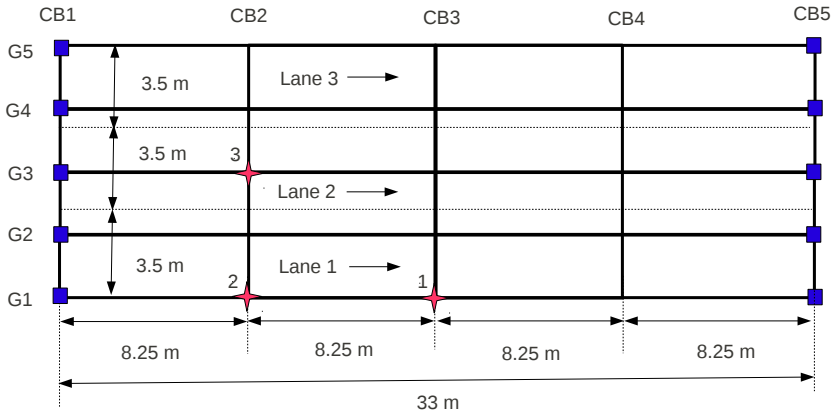

Figure 3: Scheme of bridge details.

results are consistent with the theoretical modal analysis based on a finite element model of the deck bridge [7].

3 EXPERIMENTAL STUDY OF ENERGY HARVESTING PERFORMANCE

A piezoelectric energy harvesting device was designed for investigating operational conditions and comparing the measured performances with theoretical predictions. The main design requirement was to tune the resonant frequency of the inertial harvester close to 14.5 Hz, thus targeting the resonant vibration of the pipe identified in Section 2.3. That requirement did not match the specifications of commercial energy harvesters, which are generally designed for frequencies above 30 Hz. The piezoelectric harvester that was devised is of the cantilever type. Two bimorph piezoelectric patches Midé QP20W were bonded on the upper and lower surface of a $40\times220\times0.8$ mm^3 steel plate. Those bimorph piezoelectric patches were bonded at the clamped end side of the plate. An additional 12 g concentrated mass was placed on the steel surface for tuning the resonant frequency of the oscillator. A picture of the device is displayed in Figure 7. The material parameters provided in the manufacturer's datasheet are reported in Table 1 (E_p and E_e are respectively the Young modulus of the piezoelectric material and of the epoxy, ρ_p and ρ_e are the mass densities, e_{31} is the piezoelectric constant, ϵ^s_{33} is the relative permittivity at constant strain).

The experimental test set-up is shown in Figure 7(right). A first series of tests (that we do not fully report here) consisted in applying known harmonic base excitations to the

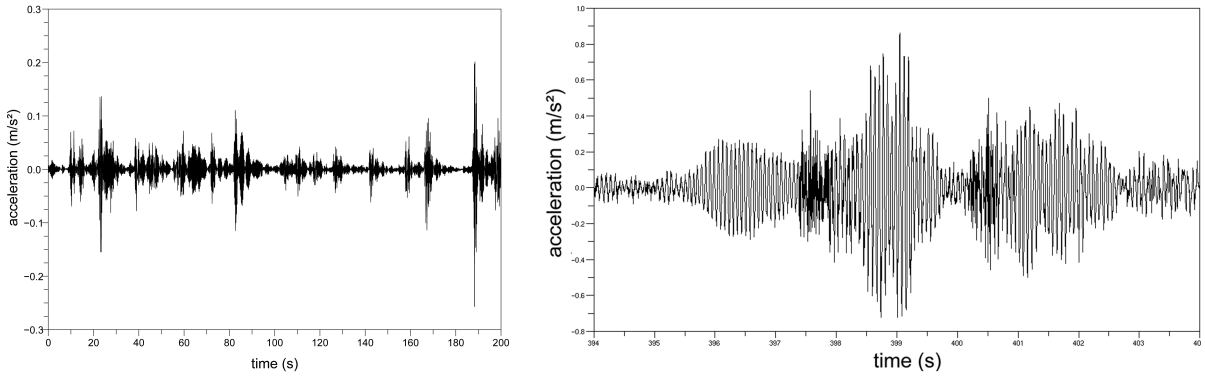

Figure 4: Recorded traffic induced acceleration measured at mid-span on girder 1 (left) and on a water pipe on girder 1 (right).

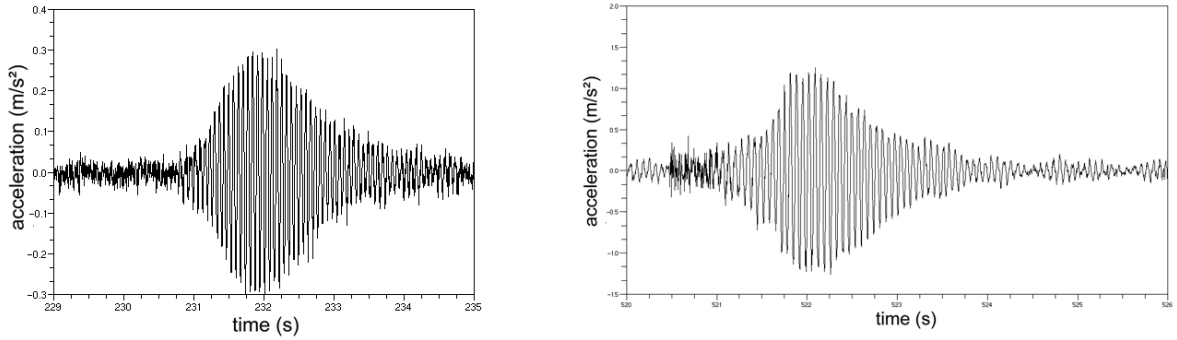

Figure 5: Examples of burst excitation due to a single lorry.

Table 1: Material parameters of the piezoelectric patch.

E_p	E_e	e_{31}	ϵ_{33}^s	ρ_p	ρ_e
MPa		$\mathrm{C.m^{-2}}$		$\mathrm{kg.m^{-3}}$	$\mathrm{kg.m^{-3}}$
69000	5000	13.1	1700	7800	8000

harvester. Tests were first carried out with a pure resistive load $R = 100$ kΩ connected to the output of the piezoelectric electrodes wired in series. In those tests, the RMS amplitude of the harmonic excitation was set to 0.2 $\mathrm{m.s^{-2}}$. The device was found to have a resonant frequency close to 14.4 Hz and the maximum measured value of power was 0.19 mW.

Similar tests were subsequently performed by replacing the resistive load R with an ALD EH300 circuit. That circuit provides a controlled voltage between 1.8 and 3.6 V through a storage capacitor, and can be used to power microelectronic devices. The energy E^{EH} accumulated during one loading cycle of the capacitor is given by $E^{EH} =$

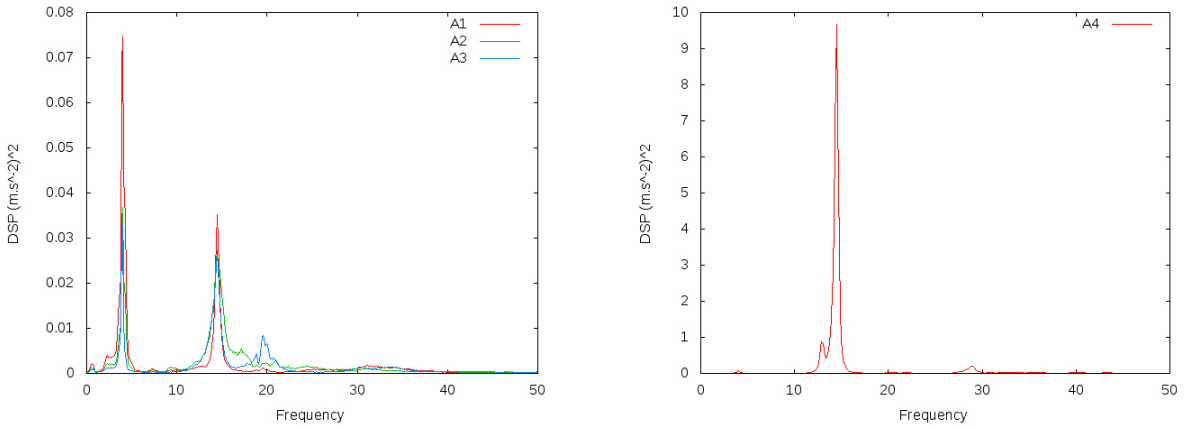

Figure 6: Power spectral densities of measured accelerations at different locations on the girders(left) and on the pipe fixed on girder 1 (right).

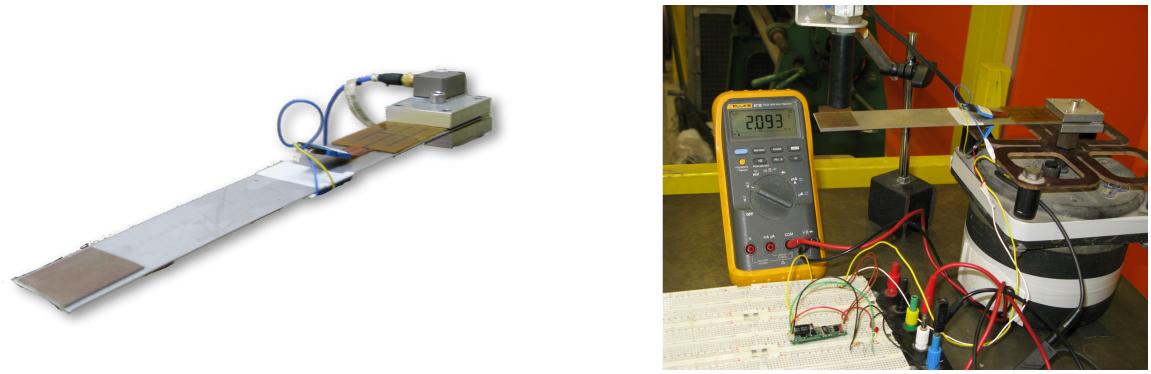

Figure 7: Piezoelectric harvester designed for traffic-induced vibrations (left), and view of the test set-up (right).

$C^{EH}(V_1^2 - V_0^2)/2$ where $V_0 = 1.8$ V, $V_1 = 3.6$ V, and C^{EH} is the storage capacity. The time ΔT for charging the capacitor between 1.8 V and 3.6 V in stationary harmonic regime was measured and the related mean power P^{EH} was evaluated by the formula $P^{EH} = E^{EH}/\Delta T$. The efficiency of the EH300 circuit can be estimated by calculating the ratio $\eta = P^{EH}/P^R$ between P^{EH} and the average power P^R obtained for a purely resisitive load $R = 100$ kΩ. In a first approximation, the ratio $\eta = P^{EH}/P^R$ is constant near the resonance and equal to 0.6 (see [8] for additional details).

The most interesting tests were carried out by replacing the harmonic excitation with the excitation measured on the pipe. An example of record of the output voltage of the EH300 circuit for a real acceleration traffic excitation is shown in Figure 8. In order to check the sensitivity of the device to the frequency tuning in operational conditions, several

tests were performed by slightly changing the resonant frequency of the oscillator. The results are shown in Figure 9. As could be expected, the harvested power is dramatically lower than for an harmonic excitation of the same RMS value. In good tuning conditions, the harvested power was about 0.029 mW.

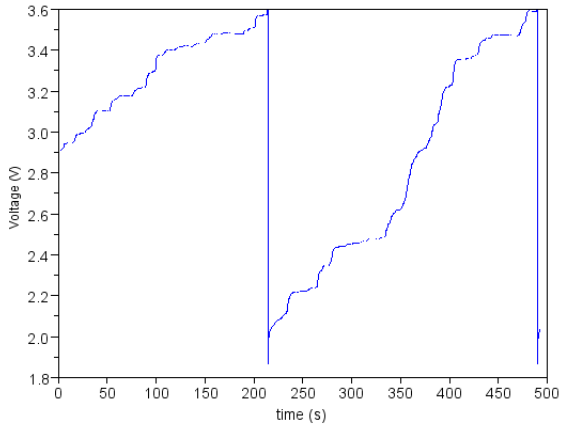

Figure 8: Storage capacity output voltage in the case of traffic induced excitation.

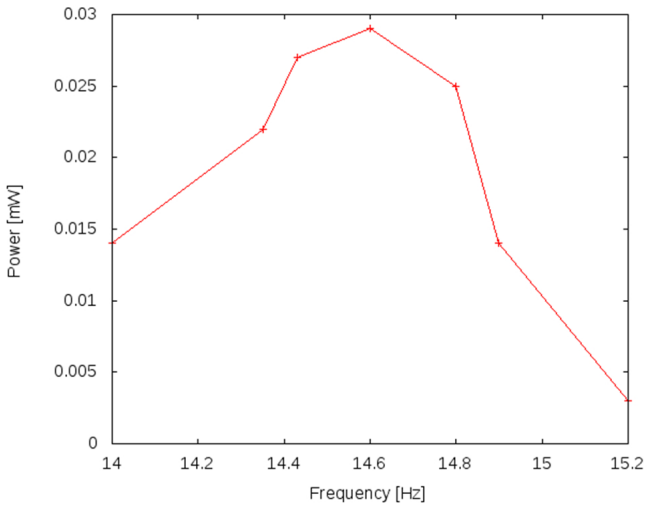

Figure 9: Harvested power using the EH300 circuit. Case of traffic induced excitation.

Table 2: Lumped model parameters.

m (g)	k (N.m^{-1})	c (N.s.m^{-1})	θ (N.V^{-1})	m^* (g)	C_p (nF)
23	188	0.02	2.34 10^{-4}	21.4	2.24

4 MODEL OF POWER CONVERSION FOR TRAFFIC-INDUCED EXCITATIONS

The single mode approximation of the energy harvester powering a resistive load R leads to the dynamic system model [9]:

$$\begin{aligned} &m\ddot{z} + c\dot{z} + kz - \theta v = m^* f \\ &\theta\dot{z} + C_p\dot{v} + \frac{v}{R} = 0 \end{aligned} \tag{1}$$

where $z(t)$ is the displacement at the tip of the beam, $v(t)$ is the voltage in the resistor, and $f(t)$ is the applied excitation. The values of all the system parameters are reported in Table 2 (see [8] for details on the identification of those parameters).

As presented in section 2.2, traffic-induced excitations consist of sequences of short-time pulses corresponding to individual lorries passing by. A simple model of such a pulse is obtained by considering the function

$$A\, f_0(t) \tag{2}$$

where

$$f_0(t) = \mathrm{tri}(t) \sin \omega_i t \tag{3}$$

and $\mathrm{tri}(t)$ is the triangle function defined as

$$\mathrm{tri}(t) = \begin{cases} 0 & \text{for } |t| > M \\ 1 + t/M & \text{for } -M \leq t \leq 0 \\ 1 - t/M & \text{for } 0 \leq t \leq M \end{cases} \tag{4}$$

That model is compatible with the experimental observations of section 2.2, and simple enough for the most of the subsequent analysis to be performed in closed-form. In (2), the parameter M characterizes the duration of the pulse and A is the peak level.

Consider a train of pulses, i.e. an acceleration signal $f(t)$ of the form

$$f(t) = \sum_{k=-\infty}^{+\infty} A_k f_0(t - t_k) \tag{5}$$

For such a non periodic excitation, the harvester power P^R is obtained by calculating the average power on the time interval $[-T/2, T/2]$ and taking the limit $T \to +\infty$. More

precisely, for any $T > 0$ we consider the truncated signal $f_T(t)$ defined as $f_T(t) = f(t)$ if $|t| \leq T/2$, and $f_T(t) = 0$ otherwise. Let V_T be the solution of (1) for the input acceleration f_T. The Fourier transform $\hat{V}_T$ of V_T is given by

$$\hat{V}_T(\omega) = \frac{\hat{f}_T(\omega)}{H(\omega)} \tag{6}$$

where

$$H(\omega) = \frac{1}{\theta}(-C_p(\omega_0^2 - \omega^2) - \frac{\nu}{R}) - \frac{\theta}{m} + \frac{i}{\theta}(\frac{\omega_0^2 - \omega^2}{R\omega} - \omega\nu C_p) \tag{7}$$

The average harvested power P^R is given by

$$P^R = \lim_{T\to+\infty} \frac{1}{T} \int_{-\infty}^{\infty} \frac{V_T^2(t)}{R} dt \tag{8}$$

Combining Parseval theorem with (6), we obtain

$$P^R = \lim_{T\to+\infty} \frac{1}{2\pi T} \int_{-\infty}^{\infty} \frac{|\hat{f}_T(\omega)|^2}{|H(\omega)|^2} d\omega \tag{9}$$

Let us now assume that A_k and t_k in (5) are random variables. We use brackets $\langle\ \rangle$ to denote ensemble averages. We further assume that the variables A_k are uncorrelated. From (9) we obtain

$$\langle P^R \rangle = \frac{1}{2\pi} \int_{-\infty}^{\infty} \frac{S_f(\omega)}{|H(\omega)|^2} d\omega \tag{10}$$

where S_f is the power spectral density of f, defined as

$$S_f(\omega) = \lim_{T\to+\infty} \frac{\langle |\hat{f}_T(\omega)|^2 \rangle}{T} \tag{11}$$

We refer to the textbooks of Drake [10] and Mix [11] for more details on random signal theory. As detailed in [8], the average harvested power is given by

$$\langle P^R \rangle = N \langle A^2 \rangle E_0 \tag{12}$$

where N is the average rate of pulse emission, and

$$E_0 = \frac{1}{2\pi R} \int_{-\infty}^{+\infty} \frac{|\hat{f}_0(\omega)|^2}{|H(\omega)|^2} d\omega \tag{13}$$

.

In night-time, the experimental measurements show that the average delay between two lorries is 18 s. Using that value in (12) gives a power of 10.1 μW. In order to check that estimate, we have numerically performed a Fast Fourier Transform (FFT) of the

acceleration signal to obtain the power. That procedure yields a power of 13.5 μW, which is of the same order of magnitude as the result of (12) .

In day time, the average delay between two trucks is measured to be 3.6 s. Calculating the power via a FFT of the day-time acceleration signal leads to a power of 59.8 μW, roughly five times bigger than in night time conditions. Using the formula (12) gives a power of 50μW, which again is of the same order of magnitude as the value obtained by FFT of the full signal.

All the considerations so far apply to a purely resistive load R. If we now consider that a EH300 circuit is used, then the harvested power P^{EH} can be estimated as $P^{EH} = \eta P^R$ where η characterizes the relative efficiency of the circuit compared to the reference resistance R. The efficiency η has been assessed in section 3, leading to $\eta = 0.6$ for R=100 kΩ. Using the formula (12) , we end up with the following estimate:

$$\langle P^{EH} \rangle = \eta N \langle A^2 \rangle E_0 \tag{14}$$

The curve in Figure 10 shows the power given by (14) as a function of the resonant frequency ω_0. That curve is to be compared with the experimental measurements of Figure 9, showing good agreement. In particular, the simplified formula (14) gives a good estimate of the maximum harvested power, which is close to 0.03 mW. The formula (14) also captures the increased bandwidth compared to the case of harmonic excitations: the half-power bandwidth in Figure 10 is indeed approximatively equal to 0.8 Hz, as in Figure 9)

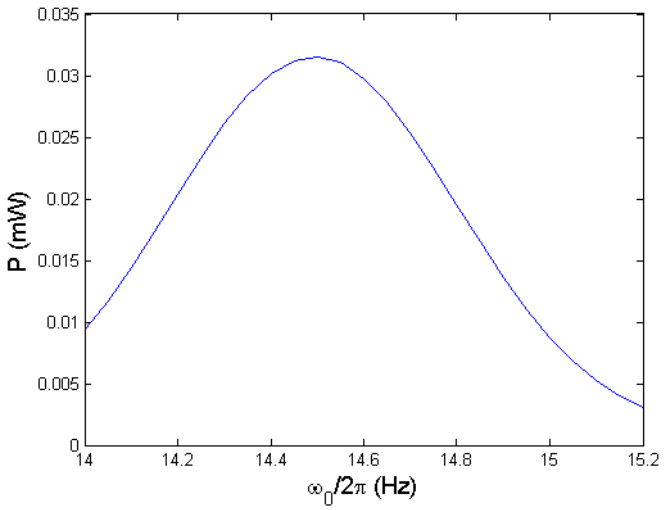

Figure 10: Prediction of the harvested power for traffic-induced excitation, as a function of the resonant frequency.

5 CONCLUSION

The study of in situ measurements shows that traffic-induced vibrations in bridges consist in random train of short-time pulses. The detailed structure of those pulses notably depends on the location considered and on the modal response of the bridge. The cantilever piezoelectric harvester that has been presented in this paper targets a transverse bending mode of the bridge, corresponding to a frequency of 14.5 Hz. For peak traffic intensity, power up to 0.03 mW can be produced, with a controlled voltage between 1.8 and 3.6 V. That energy supply could be used to power wireless health monitoring sensor nodes with low cycle duty. A simple model for piezoelectric harvester under non-periodic and random excitations has been studied, leading to a simple formula relating the harvested power to traffic statistics and to the constitutive parameters of the piezoelectric device. That formula is found to agree relatively well with experimental measurements under operating conditions, and could be used as a design rule for piezoelectric harvesters fitted to bridges. In that regard, we note that the presented piezoelectric device is not necessarily optimal: more advanced design could possibly result in a better energy production / device volume ratio.

Acknowledgements

The authors are grateful to the SANEF authorities of the tested bridge for the provided support. The authors wish to thank Jean-Luc Bachelier and René-Stéphane Morelle for their help in setting up the experiments. The contribution of Erick Merliot to the finite element analysis is also gratefully acknowledged.

REFERENCES

[1] E.K. Reilly, F. Burghardt, R. Fain, and P. Wright. Powering a wireless sensor node with a vibration-driven piezoelectric energy harvester. *Smart Materials and Structures*, 20:125006, 2011.

[2] C.B. Williams, A. Pavic, R.S. Crouch, R.C. Woods, et al. Feasibility study of vibration-electric generator for bridge vibration sensors. In *Society for Experimental Mechanics, Inc, 16 th International Modal Analysis Conference.*, volume 2, pages 1111–1117, 1998.

[3] C.B. Williams and R.B. Yates. Analysis of a micro-electric generator for microsystems. *Sensors and Actuators A: Physical*, 52(1):8–11, 1996.

[4] S.F. Ali, M.I. Friswell, and S. Adhikari. Analysis of energy harvesters for highway bridges. *Journal of Intelligent Material Systems and Structures*, 22(16):1929–1938, 2011.

[5] D. Siegert, M. Estivin, J. Billo, F.X. Barin, and F. Toutlemonde. Extreme effect of traffic loads on a prestressed concrete bridge. In *Proceeding of the International Conference on Heavy Vehicle, Paris*, 2008.

[6] D. Siegert, L. Mevel, E. Reynders, G. De Roeck, and M. Goursat. Variation of modal parameter estimates of a prestressed concrete bridge. In *27th International Modal Analysis Conference (IMAC-XXVII)*, 2009.

[7] E. Balmes, M. Corus, D. Siegert, et al. Modeling thermal effects on bridge dynamic responses. In *Proceedings of the 24th International Modal Analysis Conference (IMAC-XXIV)*, 2006.

[8] M. Peigney and D. Siegert. Piezoelectric energy harvesting from traffic-induced bridge vibrations. *Smart Materials and Structures*, 22(9):095019, 2013.

[9] N.E. Dutoit, L.W. Brian, and K. Sang-Gook. Design considerations for MEMS-scale piezoelectric mechanical vibration energy harvesters. *Integrated Ferroelectrics*, 71(1):121–160, 2005.

[10] A.W. Drake. *Fundamentals of Applied Probability Theory*. McGraw-Hill, New York, 1988.

[11] D.F. Mix. *Random Signal Processing*. Prentice Hall, Englewood Cliffs, 1995.